

A study of properties of ZrO_2 thin films deposited by magnetron sputtering under different plasma parameters: Biomedical application

Hind Zegtouf^{*}, Nadia Saoula^{**}, Mourad Azibi^{**}, Larbi Bait^{**},
 Nouredine Madaoui^{**}, Mohamed Redha
 Khelladi^{***}, Mohamed Kechouane^{*}

ZrO_2 thin films were deposited on 316L stainless steel substrate by a radio-frequency magnetron sputtering system. The substrate bias voltage, the working gas rate and the reactive gas fraction in the gas mixture were varied. These variations produce a variation in the deferent properties of the obtained films. The deposited films were characterized by X-Rays Diffraction, Atomic Force Microscopy, nano-indentation and potentio-dynamic polarization. The experimental results show that the film thickness and the roughness of the films are highly influenced by the plasma parameters. XRD results show that the monoclinic phase is predominant in unbiased deposited films. The best anti-corrosion performance and hardness were obtained for ZrO_2 deposited with a substrate bias voltage of -75 V, Ar rate of 6 sccm and oxygen fraction of 25%.

Key words: ZrO_2 , magnetron sputtering, thin films, hardness, corrosion

1 Introduction

Zirconia (ZrO_2) is a metal dioxide known for its unique properties such as inertness, biocompatibility, along with mechanical strength and toughness, coupled with Young's modulus similar to stainless steels, which makes it a good choice for many applications. In order to be used as a biomaterial, materials need to be 'inert' to prevent any biological rejection. They should also have sufficient mechanical strength and more importantly, very high corrosion and wear resistance in the highly corrosive body environment [1]. Stainless Steel is regarded as one of the most suitable materials for the manufacture in the medical industry for biomedical implants [2]. However, an acceleration of the fatigue failure of type 316 stainless steel is observed in simulated body fluids relative to that of air [3]. The modification of the surface or depositing films such as ZrO_2 could be the solution to solve this problem [2].

Magnetron sputtering is widely used for the deposition of various range on thin films on many types of substrates because of its ability to achieve a high rate and good quality film properties [4]. The different properties of the films can be controlled by the sputtering parameters: reactive gases [5], deposition rate [6], deposition temperature [5] and the negative substrate bias voltage [7]. The latter is considered as a critical parameter, because it allows to control the energy of the ions bombardment on the substrate witch can affect the properties of

the deposited films [2]. In this study, ZrO_2 thin films are deposited by radio-frequency magnetron sputtering (RFMS) process on stainless steel (316L). The negative bias voltage [0 to -75 V] was applied to the substrate in order to investigate the effect of ion bombardment on the growth of ZrO_2 films. In addition, the objective of this work was to study the effect of the bias voltage applied to the substrate (Vs), the working gas rate and the reactive gas fraction on the corrosion and mechanical properties of ZrO_2 films.

2 Experimental details

2.1 Coating deposition

In this work zirconia thin films were deposited on cylindrical 316L stainless steel; Fig. 1(a): thickness of 8 mm and diameter of 10 mm. The working faces of the samples were polished until their surfaces became smooth and mirror-like bright, Fig. 1(b), then they were ultrasonically cleaned in acetone and ethanol and subsequently dried prior to the deposition process. Finally, The ZrO_2 films were deposited by radio-frequency (13.56 MHz) magnetron sputtering at room temperature using a sputtering system which is described in Fig. 1(c). The sputtering cathode was thick pure zirconium target. This latter is distanced from the substrate holder (diameter 100 mm) by 30 mm. The gases used are high-purity argon

^{*}Laboratoire Physique des Matériaux, Faculté de Physique, USTHB, BP 32 El Alia 16111 Bab Ezzouar, Algiers, Algeria, ^{**}Division Milieux Ionisés et Lasers, Centre de Développement des Technologies Avancées, CDTA, Cité du 20 aout 1956, Baba Hassen, BP no. 17, Algiers Algeria, nsaoula@cdta.dz, ^{***}Laboratoire de Chimie, Ingénierie Moléculaire et Nanostructures. Université Ferhat Abbas-Sétif 1, 19000 Sétif, Algeria

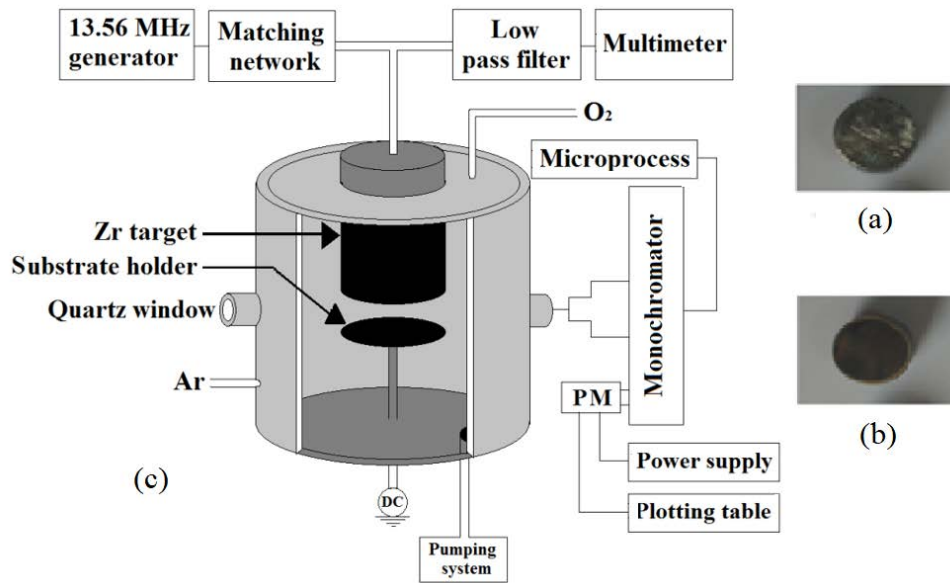


Fig. 1. Experimental setup: (a) – pre-polished substrate, (b) – polished substrate, and (c) – sputtering system

Table 1. Sputtering conditions for the deposition of ZrO₂ thin films

Samples	Target-substrate distance	Substrate bias voltage (V)	Ar rate	Reactive gas fraction (O ₂) (%)	Working gas pressure	Sputtering power	Deposition time
S1	30 mm	0	20 sccm	15	20 mTorr	250 W	50 min
S2		0		25			
S3		0	25				
S4		-75	6 sccm	25			

Target: Pure Zr (99.99%), Base Pressure: 1.0×10^{-6} Torr

(99.99990%) as the working gas and mixture of oxygen (99.99%) as a reactive gas. Argon and oxygen flow rates were controlled separately using mass flow controllers. The sputtering chamber was evacuated to less than 10^{-6} Torr before introducing the gases into the chamber. The flow rate of O₂ was set as 15 and 25% of the gas mixture of Ar + O₂ while the substrate bias voltage that was applied to the substrate was changed by 0 and -75 V. The detailed deposition conditions are listed in Table 1. In all the runs, the substrate was not heated.

2.2 Chemical and physical analyses

To investigate the structure of obtained thin films, XRD measurements were carried out using a Bruker AXS D8 Advance diffractometer in Bragg-Brentano geometry ($\theta-2\theta$ geometry) with CuK α radiation. The morphology of the films was studied by using an atomic force microscope (type: MFP-3D from Asylum Research an Oxford Instruments company). The film thicknesses were measured from cross-sectional scanning electron microscopy (SEM) micrographs. The micro-hardness of the films was measured by the dynamical micro-indentation method

with a Nano-test 550 instrument. The load-penetration curves were obtained using a Berkovich diamond indenter and hardness values were deduced by the Oliver and Pharr analysis method [8]. The corrosion resistance of ZrO₂ coatings was evaluated by potentiodynamic polarization test using a PARSTAT 4000 (Princeton Applied Research, NJ, USA) potentiostat/Galvanostat with its VesaStudio software.

3 Results and discussions

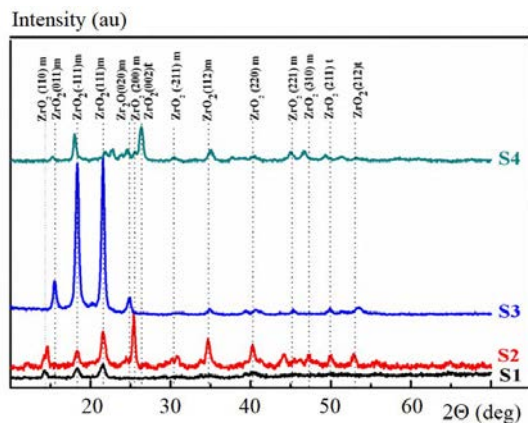
3.1 Structure and morphology

The XRD patterns of the ZrO₂ deposited films are shown in Fig. 2. These patterns confirm the crystallization of the obtained films. For the deposited films with no bias applied to the substrate (0 V), the most intense peaks observed are specific of the monoclinic phase which is the most stable phase of ZrO₂. While S1 and S3 showed a preferred orientation to (111) of the monoclinic phase, the preferred orientation of S2 was (002) of the monoclinic phase. When a bias was applied to the substrate (-75

Table 2. Deposition rate, structural and morphological properties of the ZrO₂ deposited films

Samples	Orientation	Deposition rate	Thickness	Roughness	Residual stress	FWHM	Grain size
		($\mu\text{m}/\text{min}$)	(μm)	(nm)	(GPa)	($^\circ$)	(nm)
S1	111 m	0.011	0.55	4.2	0.71	0.55	14.92
S2	200 m	0.008	0.42	12.1	1.77	0.36	23.34
S3	111 m	0.020	1.00	13.8	0.93	0.40	20.52
S4	002 t	0.015	0.75	4.1	22.32	0.45	18.56

V), mixture phases of monoclinic and tetragonal ZrO₂ phases are observed in S4. These results show that the texture of the films is very sensitive to the substrate bias, the Ar rate and the O₂ fraction. These results show that the crystallization of the deposited films increases with the increase of oxygen fraction in the Ar + O₂ mixture, the decrease of the Ar rate in the deposition chamber, and the decrease of substrate bias voltage. In A similar study that was done by Wong and *et al*[9], ZrO₂ was confirmed to be highly resistant to damage caused by ion bombardment [9].

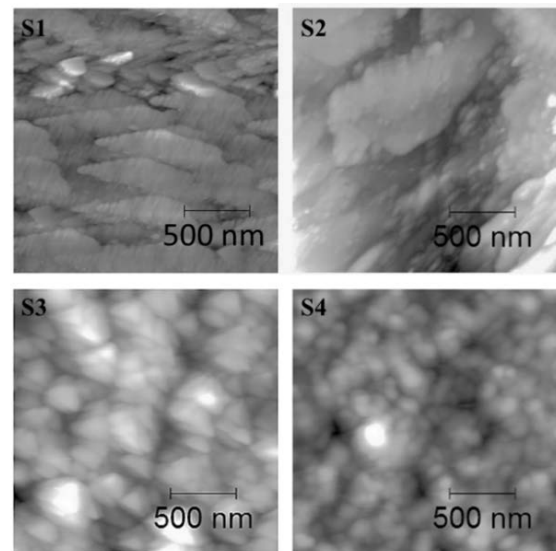
**Fig. 2.** XRD diffraction patterns of ZrO₂ films obtained for different samples (m: monoclinic, t: tetragonal, c: cubic, h: hexagonal)

The mean crystallite size (D) of ZrO₂ thin films was calculated from the Debye equation, [10]

$$D = \frac{0.94\lambda}{\beta \cos \theta} \quad (1)$$

where λ , β and θ are the incident wave-length of the X-ray (for Cu, $K\alpha = 1.54056 \text{ \AA}$), the full width at half maximum (FWHM) of the peak intensity in radian, and the Bragg angle of the mean diffraction peak, respectively. The results of the calculations are given in Table 2. The grain size increases with the increase of the oxygen fraction and Ar rate while it decreases with the increase of the substrate bias voltage which can explain the phase transformation from monoclinic to tetragonal for S4. According to Ji *et al*[11], the high-temperature tetragonal phase can be maintained in pure zirconia at room temperature by adding a stabilizer, high pressures or producing material with very small grain sizes with a critical diameter of

30 nm. They explain the size effect regarding the higher surface energy of the stable monoclinic phase compared with that of the tetragonal phase [11]. The thickness of the film was obtained from a cross-sectional SEM image of the film. It decreases with the increase of the oxygen fraction and Ar rate. According to J. Park *et al*[12], the increase of the oxygen fraction would lead to the decrease of the sputtering yield, and as a result, the thickness of the films would decrease. The film thickness is decreased with increasing of the applied substrate bias voltage. That's could be due to volume change that happened during the phase transformation.

**Fig. 3.** AFM micrographs of ZrO₂ films obtained for different samples

The surface morphology of the films of S1 with 15% of O₂ is notably smoother than that of the films of S2 with 25% of O₂ as seen in Fig. 3. Table 2 presents the root-mean-square (rms) surface roughness, acquired by AFM of the different samples. These results are in a good agreement with the ones obtained by C. Y. Ma *et al*[13]. They showed that the increase of the surface roughness with the increase of the oxygen partial pressure is approximately linear. AFM surface images are shown in Fig. 3. The deposited films of S3 at 0 V exhibited triangular columnar structure which loses its triangular form and becomes smoother, smaller granular size and less rough with the increase of the substrate bias voltage

to -75 V. When a negative bias voltage is applied to the substrates, the ion bombardment increases; which reduces the nucleation energy and giving rise to the variations in the surface morphology and microstructures of the thin films [14].

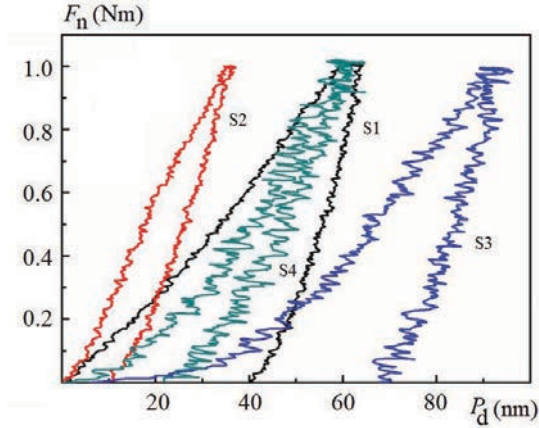


Fig. 4. Penetration curves of the indenter in ZrO₂ thin films

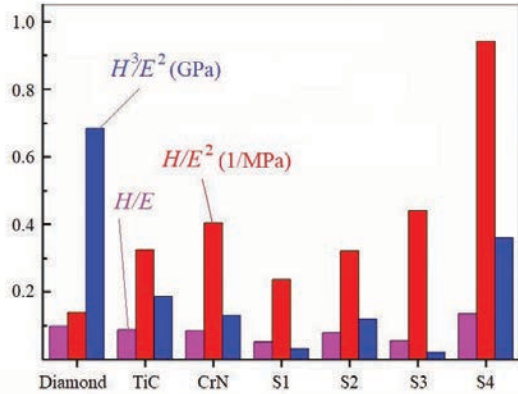


Fig. 5. H/E , H/E^2 and H^3/E^2 of the deposited films, diamond [17], TiC [18] and CrN [19] that was calculated from the hardness and young modulus of measured and literature values

3.2 Mechanical properties

The mechanical properties of the deposited films were investigated by nanoindentation with continuous stiffness measurement (CSM) method. Figure 4 shows the force-penetration curves for all the ZrO₂ thin films, which reflects the general deformation behavior during the penetration of a Berkovich indenter loaded with CSM mode. Figure 4 confirms the resistance of the deposited films to mechanical stresses. The obtained values of the Young modulus are (S1): 221 GPa, (S2): 245 GPa, (S3): 125 GPa and (S4): 144 GPa. The obtained values of the hardness are (S1): 11.5 GPa, (S2): 19.3 GPa, (S3): 6.87 GPa and (S4): 19.54 GPa. The mean three H to E ratios that influence the wear resistance of a material are: H/E , [2], which characterizes the resistance of the material to elastic deformation, H/E^2 indicates material ability to resist permanent damage [15] and H^3/E^2 which allows estimating the materia ability to dissipate energy at plastic deformation during loading [16]. The samples of this

study show very interesting H/E , H/E^2 and H^3/E^2 ratios as presented in Fig. 5 with a maximum H/E , H/E^2 and H^3/E^2 ratio of 0.13575, 0.94232 and 0.36005 are found for sample 4, respectively. These values are close to the values usually obtained for hard covalent materials such as TiC, and CrN ($0.02 \leq H^3/E^2 \leq 0.33$; 0.91 GPa for the diamond is the most important value).

3.3 Electrochemical properties

The electrochemical behavior of the ZrO₂ deposited films on 316L stainless steel was studied in a physiological environment (Hank's Solution). Tafel extrapolation and polarization resistance are the methods to measure electrochemical parameters. For an electrochemical reaction under activation control, polarization curves exhibit linear behavior in the $\log i$ vs E plots called Tafel's behavior. The equation Tafel's law is $E = a + b \log i$, where a and b are constants [20].

The obtained results of the potentiodynamic polarization curves $\log i = f(E)$ are shown in Fig. 6. We notice a positive shift of the global polarization curves of the samples deposited under substrate bias with a cathodic shift of their corrosion potential. Suggesting that there is a formation of corrosion products on the surface of the sample [21]. Electrochemical parameters such as corrosion potential (E_{corr}), corrosion current density (i_{corr}), corrosion rate and polarization resistance (R_p) were calculated and shown in Table 3. We notice that there is an increase in the corrosion potential with the rise of substrate bias: from -121 mV for 0 V (S3) to -225 mV for -75 V (S4) while the samples deposited with higher Ar rate (S1, S2) present higher values of the corrosion potential and porosity. The corrosion resistance reaches a value of 0.1294 M Ω for a polarization of -75 V which is higher than the ones obtained for the uncoated substrate with a corrosion rate (0.88135 mpy). These results show that the obtained films for the highest substrate bias (-75 V) are more protective than the uncoated steel. The corrosion resistance is a very important feature in the choice of metallic biomaterials.

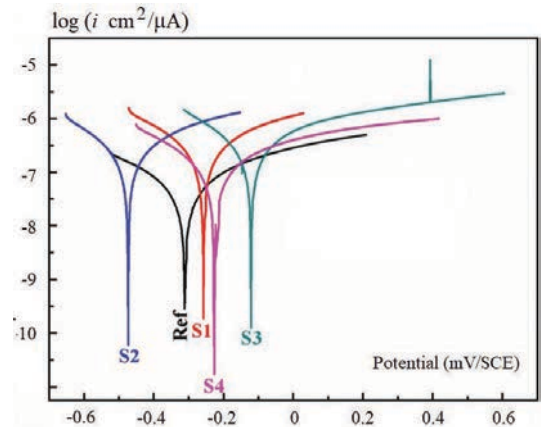


Fig. 6. Effect of substrate bias voltage on the polarization curves of ZrO₂/316L thin films and uncoated Steel in Hank's solution

Table 3. Electrochemical parameters of potentiodynamic polarization tests for stainless steel with and without a thin film of ZrO₂ in Hank's Solution

Samples	Corrosion Rate (mpy)	R_p (M Ω)	E_{corr} (mV)	i_{corr} (nA)	Porosity
Stainless steel 316L	0.881	0.139	-550.88	275.76	-
S1	0.578	0.216	-258.326	823.197	0.407
S2	0.399	0.046	-473.903	567.389	2.627
S3	1.523	0.327	-121.13	671.45	0.218
S4	0.278	0.435	-224.85	91.89	0.192

4 Conclusions

In this paper, we describe the effect of the plasma parameters on the properties of zirconia (ZrO₂) deposited on stainless steel using RF magnetron sputtering system. It was evident that zirconia films deposited consisted of poly-crystalline phase of monoclinic and tetragonal.

The study shows that the plasma parameters have a great effect on the electrochemical nature of the films. The zirconia film deposited at -75 V shows optimum mechanical and electrochemical properties. The optimum oxygen fraction for ZrO₂ deposition is 25%. And the optimum Ar rate is 6 sccm.

REFERENCES

- [1] G. Manivasagam, D. Dhinasekaran, A. Rajamanickam, "Biomedical Implants: Corrosion and its Prevention-A Review", *Recent Patents on Corrosion Science*, vol. 2, pp. 40-54, 2010.
- [2] L. Bait, L. Azouz, N. Madaoui, N. Saoula, "Influence of substrate bias voltage on the properties of TiO₂ deposited by radio-frequency magnetron sputtering on 304L for biomaterials applications", *Applied Surface Science*, vol. 72, pp. 395-397, 2017.
- [3] K. Wheeler, L. James, "Fatigue behavior of type 316 stainless steel under simulated body conditions", *Journal of Biomedical Materials Research Part A*, vol. 267, pp. 81-85, 1971.
- [4] V. Vancoppenolle, P.-Y. Jouan, A. Ricard, M. Wautelet, J.-P. Dauchot, M. Hecq, "Oxygen active species in an Ar-O₂ magnetron discharge for titanium oxide deposition", *Applied Surface Science*, vol. 249, pp. 205-255, 2003.
- [5] N. Li, M. Suzuki, Y. Abe, M. Kawamura, K. Sasaki, H. Itoh, *et al*, "Effects of substrate temperature on the ion conductivity of hydrated ZrO₂ thin films prepared by reactive sputtering in H₂O atmosphere", *Solar Energy Materials and Solar Cells*, vol. 160, pp. 95-99, 2012.
- [6] J. Vlček, J. Rezek, J. Houška, R. Čerstvý, R. Bugyi, "Process stabilization and a significant enhancement of the deposition rate in reactive high-power impulse magnetron sputtering of ZrO₂ and Ta₂O₅ films", *Surface and Coatings Technology*, vol. 236, pp. 550-556, 2013.
- [7] S. Zhao, F. Ma, K. Xu, H. Liang, "Optical properties and structural characterization of bias sputtered ZrO₂ films", *Journal of Alloys and Compounds*, vol. 453, pp. 453-457, 2008.
- [8] W. C. Oliver, G. M. Pharr, "An improved technique for determining hardness and elastic modulus using load and displacement sensing indentation experiments", *Journal of materials research*, vol. 7, pp. 1564-1583, 1992.
- [9] M. Wong, W. Chia, J. Schneider, P. Yashar, W. Sproul, S. Barnett, "High-Rate Reactive DC Magnetron Sputtering of ZrO_x", *Surface and Coatings Technology*, vol. 86-87, pp. 381-387, 1996.
- [10] A. Thaveedetrakul, N. Witit-anun, V. Boonamnuyvitaya, "The role of target-to-substrate distance on the DC magnetron sputtered zirconia thin films bioactivity", *Applied Surface Science*, vol. 258, pp. 2612-2619, 2012.
- [11] Z. Ji, J. Haynes, M. Ferber, J. Rigsbee, "Metastable tetragonal zirconia formation and transformation in reactively sputter deposited zirconia coatings", *Surface and Coatings Technology*, vol. 135, pp. 109-117, 2001.
- [12] J. Park, J. K. Heo, Y.-C. Kang, "The properties of RF sputtered zirconium oxide thin films at different plasma gas ratio", *Bull Korean Chem Soc.*, vol. 31, pp. 397, 2010.
- [13] C. Ma, F. Lapostolle, P. Briois, Q. Zhang, "Effect of O₂ gas partial pressure on structures and dielectric characteristics of rf sputtered ZrO₂ thin films", *Applied surface science*, vol. 253, pp. 8718-8724, 2007.
- [14] P. Kondaiah, S. Uthanna, G. M. Rao, "Substrate bias voltage influence on structural, electronic and dielectric properties of ZrO₂ gate dielectrics", *Nanoscience, Engineering and Technology (ICONSET), International Conference on: IEEE*, pp. 616-619, 2011.
- [15] D. Joslin, W. Oliver, "A new method for analyzing data from continuous depth-sensing microindentation tests", *Journal of Materials Research*, vol. 5, pp. 123-126, 1990.
- [16] T. Tsui, G. Pharr, W. Oliver, C. Bhatia, R. White, S. Anders, *et al*, "Nanoindentation and nanoscratching of hard carbon coatings for magnetic disks", *MRS Online Proceedings Library Archive*, vol. 383, 1995.
- [17] N. Savvides, T. Bell, "Hardness and elastic modulus of diamond and diamond-like carbon films", *Thin Solid Films*, vol. 228, pp. 289-292, 1993.
- [18] T.-H. Fang, S.-R. Jian, D.-S. Chuu, "Nanomechanical properties of TiC, TiN and TiCN thin films using scanning probe microscopy and nanoindentation", *Applied Surface Science*, vol. 228, pp. 365-372, 2004.
- [19] Z. Wu, X. Tian, Z. Wang, C. Gong, S. Yang, CM. Tan, *et al*, "Microstructure and mechanical properties of CrN films fabricated by high power pulsed magnetron discharge plasma immersion ion implantation and deposition", *Applied Surface Science*, vol. 258, pp. 242-246, 2011.
- [20] E. McCafferty, "Validation of corrosion rates measured by the Tafel extrapolation method", *Corrosion Science*, vol. 47, pp. 3202-3215, 2005.
- [21] R. Kotoka, S. Yarmolenko, D. Pai, J. Sankar, "Corrosion Behavior of Reactive Sputtered Al₂O₃ and ZrO₂ Thin Films on Mg Disk Immersed in Saline Solution", *Journal of Materials Science & Technology*, vol. 31, pp. 873-880, 2015.

Received 19 March 2019